Development 138, 2523-2532 (2011) doi:10.1242/dev.062208

Drosophila Mon2 couples Oskar-induced endocytosis with actin remodeling for cortical anchorage of the germ plasm

Tsubasa Tanaka*, Yasuko Kato, Kazuki Matsuda, Kazuko Hanyu-Nakamura and Akira Nakamura†

SUMMARY

Drosophila pole (germ) plasm contains germline and abdominal determinants. Its assembly begins with the localization and translation of *oskar* (*osk*) RNA at the oocyte posterior, to which the pole plasm must be restricted for proper embryonic development. Osk stimulates endocytosis, which in turn promotes actin remodeling to form long F-actin projections at the oocyte posterior pole. Although the endocytosis-coupled actin remodeling appears to be crucial for the pole plasm anchoring, the mechanism linking Osk-induced endocytic activity and actin remodeling is unknown. Here, we report that a Golgi-endosomal protein, Mon2, acts downstream of Osk to remodel cortical actin and to anchor the pole plasm. Mon2 interacts with two actin nucleators known to be involved in *osk* RNA localization in the oocyte, Cappuccino (Capu) and Spire (Spir), and promotes the accumulation of the small GTPase Rho1 at the oocyte posterior. We also found that these actin regulators are required for Osk-dependent formation of long F-actin projections and cortical anchoring of pole plasm components. We propose that, in response to the Osk-mediated endocytic activation, vesicle-localized Mon2 acts as a scaffold that instructs the actin-remodeling complex to form long F-actin projections. This Mon2-mediated coupling event is crucial to restrict the pole plasm to the oocyte posterior cortex.

KEY WORDS: *Drosophila*, Actin dynamics, Cell polarity, Endosomes, Germ plasm, Microtubules

INTRODUCTION

In many cell types, asymmetric localization of specific RNAs and proteins is essential for exhibiting proper structure and function. These macromolecules are transported to their final destinations and anchored there. This latter step is particularly important for the long-term maintenance of cell asymmetry. A genetically tractable model for studying intracellular RNA and protein localization is the assembly of the pole (germ) plasm in *Drosophila* oocytes and embryos (Mahowald, 2001). The pole plasm is a specialized cytoplasm that contains maternal RNAs and proteins essential for germline and abdominal development. It is assembled at the posterior pole of the oocyte during oogenesis. *Drosophila* oogenesis is subdivided into 14 stages, with pole plasm assembly starting at stage 8 (Mahowald, 2001). The functional pole plasm is assembled by stage 13, stably anchored at the posterior cortex of the oocyte and later inherited by the germline progenitors (pole cells) during embryogenesis (Mahowald, 2001).

Pole plasm assembly begins with the transport of *oskar* (*osk*) RNA along microtubules to the posterior pole of the oocyte (Zimyanin et al., 2008). There, the *osk* RNA is translated, producing two isoforms, long and short Osk, by the alternate use of two in-frame translation start sites (Markussen et al., 1995). Although short Osk shares its entire sequence with long Osk, the isoforms have distinct functions in pole plasm assembly (Breitwieser et al., 1996; Markussen et al., 1995; Vanzo and Ephrussi, 2002). Downstream, short Osk recruits other pole plasm components, such as Vasa (Vas), to the oocyte posterior, presumably through direct interactions (Breitwieser et al., 1996; Markussen et al., 1995). By contrast, long Osk prevents pole plasm components from diffusing back into the cytoplasm (Vanzo and Ephrussi, 2002). Intriguingly, embryonic patterning defects are caused by either the ectopic assembly of pole plasm [elicited by Osk translation at the oocyte anterior directed by the *osk-bicoid* (*bcd*) *3′ UTR*] or the leakage of pole plasm activity into the bulk cytoplasm (induced by overexpressing *osk*) (Ephrussi and Lehmann, 1992; Smith et al., 1992). Thus, the pole plasm must be anchored at the posterior cortex for proper embryonic development.

Short and long Osk also differ in their subcellular distributions (Vanzo et al., 2007). Short Osk is located on polar granules, specialized ribonucleoprotein aggregates in the pole plasm, and long Osk is associated with endosome surfaces. Intriguingly, the oocyte posterior, where endocytosis is increased, is highly enriched with markers of early, late and recycling endosomes (Rab5, Rab7 and Rab11, respectively) (Dollar et al., 2002; Tanaka and Nakamura, 2008; Vanzo et al., 2007). *osk* oocytes, however, do not maintain either the accumulation of endosomal proteins or the increased endocytic activity at the posterior (Tanaka and Nakamura, 2008; Vanzo et al., 2007). Furthermore, the ectopic expression of long Osk at the anterior pole of the oocyte results in the anterior accumulation of endosomal proteins along with increased endocytosis (Tanaka and Nakamura, 2008). Thus, long Osk regulates endocytic activity spatially within the oocyte.

The endocytic pathway has two separate roles in pole plasm assembly (Dollar et al., 2002; Jankovics et al., 2001; Tanaka and Nakamura, 2008). First, it is required for the sustained transport of *osk* RNA by maintaining microtubule alignment. For example, in oocytes lacking Rabenosyn-5 (Rbsn-5), a Rab5 effector protein essential for endocytosis, the polarity of the microtubule array is

Laboratory for Germline Development, RIKEN Center for Developmental Biology, Kobe, Hyogo 650-0047, Japan.

*Present address: Department of Cell and Tissue Biology, University of California San Francisco, San Francisco, CA 94143-0512, USA
†Author for correspondence (akiran@cdb.riken.jp)

Accepted 23 March 2011

not maintained, disrupting *osk* RNA localization (Tanaka and Nakamura, 2008). A similar defect occurs in hypomorphic *rab11* oocytes (Dollar et al., 2002; Jankovics et al., 2001). Second, the endocytic pathway acts downstream of Osk to anchor the pole plasm components. In *rbsn-5* oocytes aberrantly expressing *osk* at the anterior, Osk and other pole plasm components diffuse from the anterior cortex into the ooplasm, indicating that endocytic activity is essential for stably anchoring them to the cortex (Tanaka and Nakamura, 2008).

The endocytic pathway is thought to anchor pole plasm components by remodeling the cortical actin cytoskeleton in response to Osk. Pole plasm anchoring is sensitive to cytochalasin D, which disrupts actin dynamics (Cha et al., 2002), and requires several actin-binding proteins, such as Moesin, Bifocal and Homer (Polesello et al., 2002; Jankovics et al., 2002; Babu et al., 2004). Osk induces long F-actin projections emanating from cortical F-actin bundles at the posterior pole of the oocyte (Vanzo et al., 2007). Ectopic F-actin projections are also induced at the anterior pole when long Osk is misexpressed at the oocyte anterior (Tanaka and Nakamura, 2008). However, when the endocytic pathway is disrupted, F-actin forms aggregates and diffuses into the ooplasm, along with pole plasm components (Tanaka and Nakamura, 2008). These observations led to the hypothesis that Osk stimulates endocytosis, which promotes actin remodeling, which in turn anchors the pole plasm components at the posterior oocyte cortex. However, the molecular mechanism linking Osk, the endocytic pathway and actin remodeling is still unknown.

Here, we identified Mon2, a conserved Golgi/endosomal protein, as an essential factor in anchoring pole plasm components at the oocyte posterior cortex. We found that oocytes lacking Mon2 did not form F-actin projections in response to Osk, but neither did they exhibit obvious defects in microtubule alignment or endocytosis. We also showed that two actin nucleators that function in *osk* RNA localization in the oocyte, Cappuccino (Capu) and Spire (Spir), play an essential role in a second aspect of pole plasm assembly: the Osk-dependent formation of long F-actin projections and cortical anchoring of pole plasm components. Finally, we found that Mon2 interacts with Capu and Spir, and promotes the accumulation of the small GTPase Rho1 at the oocyte posterior. These data support a model in which Mon2 acts as a scaffold, linking Osk-induced vesicles with these actin regulators to anchor the pole plasm to the oocyte cortex.

MATERIALS AND METHODS

Fly stocks

Flies were kept on standard cornmeal and agar medium at 25°C. The wild-type strains used were *w*; *P{neoFRT}40A* and *y w*. The transgenic and mutant stocks used were *Pvas-egfp-vas* (Sano et al., 2002), kin-β-Gal *KZ503* (Clark et al., 1994), *UASp-osk-bcd 3′ UTR* (Tanaka and Nakamura, 2008), *matα4-GAL-VP16* (Bloomington Stock Center, IN, USA), *rab5*^{2} (Wucherpfennig et al., 2003) (a gift from A. Guichet, Institut Jacques Monod, Paris, France), *Rho1*^{72F} (Strutt et al., 1997), *wimp* (Parkhurst and Ish-Horowicz, 1991), *osk*^{54} and *osk*^{150} (Kim-Ha et al., 1991).

Identification of *mon2*, *capu* and *spir* mutations

The germline clone (GLC) screen that isolated the *mon2*, *capu* and *spir* mutants was described previously (Tanaka and Nakamura, 2008). GLCs were induced using the FRT/FLP system between the *P{neoFRT}40A* and *P{Ubi-GFP(S65T)nls}2L P{neoFRT}40A* or *P{ovo*$^{D1\text{-}18}$*}2L P{neoFRT}40A* chromosomes. Mitotic recombination was induced by heat-shock of third-instar larvae at 37°C for 2 hours on two consecutive days. Chromosomal mapping for mutations was carried out as described (Tanaka and Nakamura, 2008). New alleles of *capu* and *spir* (see Fig. S2 in the supplementary material) were identified by complementation tests with *capu*^{G7} and *spir*^{RP} (Schüpbach and Wieschaus, 1991). *mon2* alleles (*B242*, *C326*, *C331*, *K388*, *K597* and *R685*) were identified by complementation tests between mutants mapped to close genetic loci. Mutation points were further determined by sequencing of PCR fragments from genomic DNAs of mutant heterozygotes.

Transgenic lines and rescue analysis

The UASp-*gfp-mon2* plasmid was constructed by cloning *gfp* and full-length *mon2* cDNA into pUASp. P-element-mediated germline transformation was carried out by standard methods using *y w* embryos as recipients. To examine whether GFP-Mon2 is functional to rescue *mon2* mutants, *y w P{hsFLP}*/*w*; *mon2 P{neoFRT}40A*/*P{ovo*$^{D1\text{-}18}$*}2L P{neoFRT}40A*; *P{matα4-GAL-VP16}*/*P{UASp-gfp-mon2}* females, in which mitotic recombination had been induced during the third-instar larval stage, were mated with *y w* males. Eggs obtained from the cross were analyzed for their ability to develop into adults. Three independent *mon2* alleles and three independent *UASp-gfp-mon2* lines were examined.

Immunofluorescence staining and endocytic assay

Immunostaining was performed by standard procedures (Tanaka and Nakamura, 2008). The primary antibodies were rabbit anti-Stau (1:3000; a gift from D. St Johnston, The Gurdon Institute, Cambridge, UK); guinea pig anti-Osk (1:3000; lab stock); rabbit anti-Osk (1:8000; a gift from A. Ephrussi, EMBL, Heidelberg, Germany); mouse anti-β-galactosidase (1:5000; Promega); rabbit anti-Rbsn-5 (1:5000), -Rab5 (1:1000), -Rab7 (1:2000 for ovaries and 1:4000 for S2 cells) and -Rab11 (1:5000 for ovaries and 1:8000 for S2 cells) (Tanaka and Nakamura, 2008); rabbit anti-Tudor (1:2000) (Amikura et al., 2001); rabbit anti-Lava Lamp (1:500; a gift from J. C. Sisson) (Sisson et al., 2000); mouse anti-p120 (1:100; Calbiochem); rabbit anti-GM130 (1:450; a gift from S. Goto) (Yano et al., 2005) and mouse anti-human Rho 3L74 (1:1000; Millipore). Alexa 488-, 568- and 660-conjugated secondary antibodies (Invitrogen) were used. DNA and F-actin were stained with DAPI and Alexa 660-conjugated phalloidin (Invitrogen), respectively. The FM4-64 incorporation assay was performed as described (Tanaka and Nakamura, 2008). Confocal images were obtained using laser confocal microscopes (Leica TCS SP2 AOBS and Olympus FV1000-D) with 63× NA 1.2 PL APO λ BL (Leica) and 60× NA 1.2 UPLSAPO (Olympus) water immersion lens. Images were processed with Adobe Photoshop.

Expression plasmids

The full-length *mon2* coding sequence (CDS) was fused with *gfp* and cloned into the pAc vector (Invitrogen), which carries the *Drosophila Actin 5c* promoter. CDSs for *capu* and *spir* were fused with the 3×FLAG-tag sequence and cloned into the pMT vector (Invitrogen), allowing copper-inducible expression from the *Metallothionein* promoter. CDSs for *Drosophila* Rab GTPases (Rab5, Rab7 and Rab11) or Rho GTPases (Rho1, RhoL, Rac1, Rac2, Cdc42 and Mtl) were cloned into pGEX5X1 (GE Healthcare) to express GST fusion proteins.

Immunoprecipitation and immunoblotting

Drosophila S2 cells were grown at 25°C in Schneider's medium (Invitrogen) supplemented with 2 mM glutamine and 10% heat-inactivated fetal calf serum. pAc-*gfp-mon2* and pMT-3×FLAG-*capu* or -*spir* were co-transfected into S2 cells using siLentFect reagent (BioRad). pMT-driven expression was induced with 0.5 mM $CuSO_4$ 2 days after transfection. Cells were then homogenized in TNG300 (50 mM Tris-HCl, pH 8.0, 300 mM NaCl, 10% glycerol, 1% Triton X-100) containing protease inhibitors (Complete EDTA-free; Roche). Pre-cleared lysates were mixed with anti-GFP agarose (MBL) and incubated for 2 hours at 4°C. The beads were washed with TNG300. Bound proteins were eluted by boiling in SDS sample buffer and analyzed by western blotting using rabbit anti-GFP (MBL) and HRP-conjugated mouse anti-Flag M2 (Sigma) antibodies. GST-tagged GTPases were expressed in *Escherichia coli* BL21 (DE3), purified using glutathione-Sepharose 4B beads (GE Healthcare), and used to evaluate the specificity of the 3L74 antibody by immunoblotting. Signal detection was performed using HRP-conjugated anti-mouse IgG (Jackson lab) and Super Signal West Dura reagent (Thermo Fisher).

Yeast two-hybrid screen

The yeast two-hybrid screen was performed using the DupLEX-A kit (Origene Technologies). The full-length *mon2* CDS was PCR-amplified and subcloned into the yeast vector pEG202-NLS to produce a bait construct (pEG-Mon2). The yeast strain EGY48, possessing pEG-Mon2 and pSH18-34, was mated with RFY206 cells that had been pre-transformed with an ovarian cDNA library in the pJG4-5 vector (provided by J. Großhans, University of Heidelberg, Heidelberg, Germany). About 1×10^6 diploid cells were screened for their galactose-dependent β-galactosidase expression and growth on plates lacking leucine. cDNA inserts in positive clones were amplified by PCR, and the 5′ ends of the inserts were sequenced. To determine the region of Mon2 that was sufficient for the interaction with Spir, deletion derivatives were constructed in pEG202-NLS.

RESULTS

Drosophila Mon2 is required for the cortical anchoring of pole plasm components

To learn more about how the pole plasm is assembled and anchored during *Drosophila* oogenesis, we conducted a germline clone (GLC) screen for ethyl methanesulfonate-induced mutations showing the abnormal localization of GFP-Vas, a fluorescent pole plasm marker (Tanaka and Nakamura, 2008). In a screen targeting chromosomal arm 2L, we identified six mutants that mapped into a single lethal complementation group, which we named *no anchor* (*noan*). In wild-type oocytes, GFP-Vas was first detectable at the posterior pole at stage 9, where it remained tightly anchored, with a progressive accumulation of protein until the end of oogenesis (Fig. 1A). In the *noan* GLC oocyte, GFP-Vas initially localized to the oocyte posterior during stages 9-10a (Fig. 1B), but its level gradually decreased, becoming undetectable in the mature oocyte (Fig. 1B). Similarly, the localization of Staufen (Stau) and Osk at the posterior pole, which occurs prior to that of Vas (Mahowald, 2001), was not maintained in the *noan* oocytes (Fig. 1C,D). Although the *noan* oocytes developed into normal-looking mature oocytes, the eggs were fragile and did not develop. Therefore, we were unable to analyze the effects of the loss of maternal *noan* activity on the formation of abdomen or germ cells in embryos. Nevertheless, these results indicated that *noan* mutations cause defective anchoring of pole plasm components to the posterior pole of the oocyte.

The genetic mapping and subsequent DNA sequencing of the *noan* locus revealed that all the *noan* alleles had a nonsense mutation in *CG8683*, which encodes a homolog of a budding yeast protein, Mon2p, also termed Ysl2p (Fig. 1E,F). Hereafter, we refer to *noan* as *mon2*. All the *mon2* alleles showed identical defects in the posterior localization of GFP-Vas with full penetrance (data not shown). As the mutation in the $mon2^{K388}$ allele was the most proximal to the translational initiation site among the six alleles identified (Fig. 1E,F), we primarily used $mon2^{K388}$ to characterize the *mon2* phenotype.

Drosophila Mon2 resides on the Golgi and endosomes

Drosophila Mon2 consists of 1684 amino acids and represents a highly conserved protein among eukaryotes. It has two Armadillo (ARM) repeat domains, which are likely to mediate protein-protein interactions, and a DUF1981 domain, which is functionally uncharacterized (Fig. 1E). In budding yeasts, *mon2* (*ysl2*) was identified as a gene whose mutation increases sensitivity to the Na^+/H^+ ionophore monensin (Murén et al., 2001), and is synthetically lethal with a mutation in *ypt51*, which encodes a Rab5 homolog (Singer-Krüger and Ferro-Novick, 1997). Yeast Mon2p (Ysl2p) forms a large protein complex on the surface of the trans-

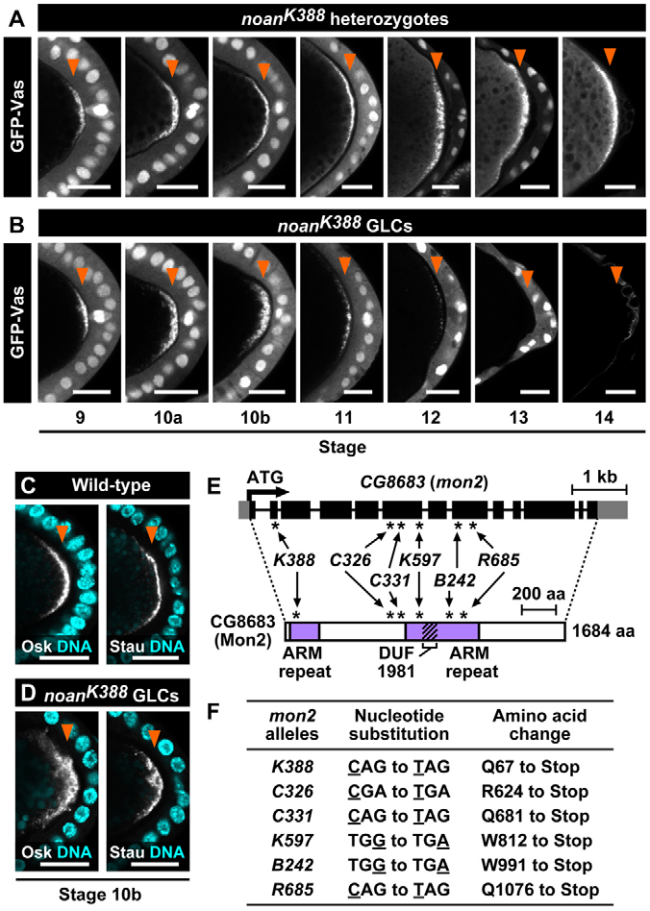

Fig. 1. Identification of the *Drosophila* Mon2 homolog. (**A-D**) Enlarged views of the posterior region of oocytes. (A,B) GFP-Vas localization in stage 9-14 oocytes of the $noan^{K388}$ heterozygous wild-type (A) and $noan^{K388}$ homozygous GLC (B) oocytes. Mutant clones lacked nuclear GFP signals in the germline. The *ubiquitin* promoter-driven nuclear GFP is visible in follicle cells surrounding the oocyte. Oocytes were staged according to Spradling (Spradling, 1993). Arrowheads indicate the posterior pole. (C,D) Localization of Osk (left panels) and Stau (right panels) in wild-type (C) and $noan^{K388}$ GLC (D) oocytes. DNA stained with DAPI is in cyan. Arrowheads indicate the posterior pole of each oocyte. In all images, anterior is to the left, posterior to the right. Scale bars: 20 μm. (**E**) The *Drosophila mon2* gene structure. The untranslated regions (UTRs), coding sequence (CDS) and introns are shown as gray boxes, black boxes and thin lines, respectively. The thick arrow indicates the translation initiation site. Below is an illustration of the domain structure of the predicted Mon2 protein, which contains two Armadillo (ARM) repeats, and within the second ARM repeat, a DUF1981 domain. The asterisks indicate the positions of mutations identified in *mon2* alleles. (**F**) Nucleotide substitutions and the corresponding amino acid changes in *mon2* alleles. Each allele had a different single nucleotide substitution that resulted in premature termination of the CDS.

Golgi network and early endosomes, and it is proposed to act as a scaffold to regulate antero- and retrograde trafficking between the Golgi, endosomes and vacuoles (Efe et al., 2005; Gillingham et al., 2006; Jochum et al., 2002; Singer-Krüger et al., 2008; Wicky et al., 2004).

Drosophila Mon2 is ubiquitously expressed, according to sequence tag and microarray expression data in FlyBase (http://flybase.org/). None of the antibodies that we generated

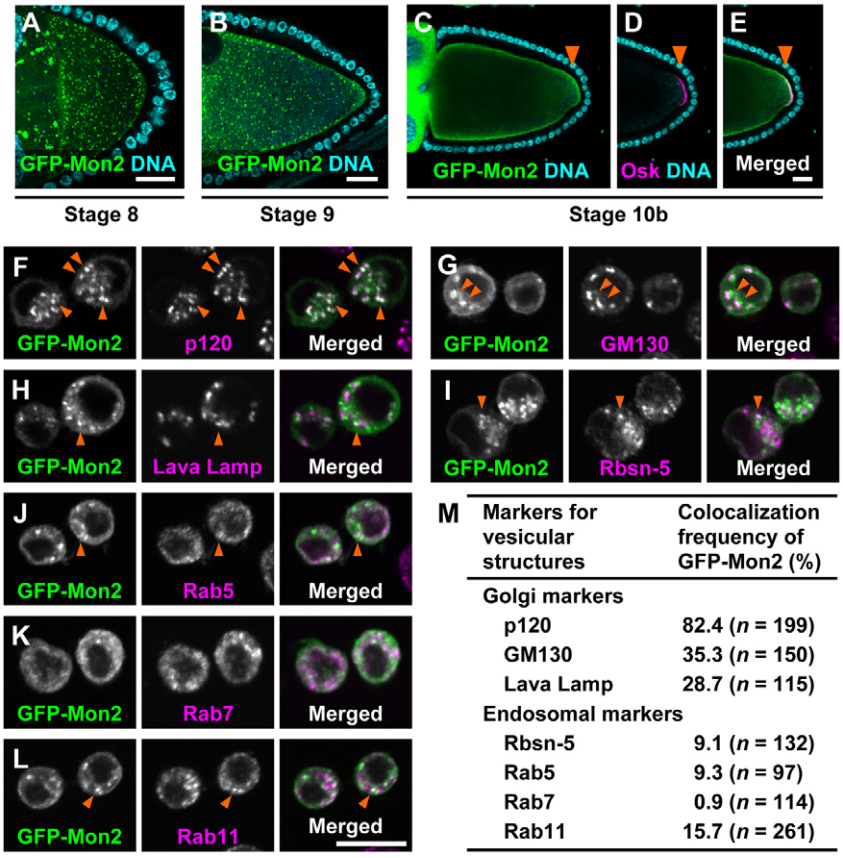

M

Markers for vesicular structures	Colocalization frequency of GFP-Mon2 (%)
Golgi markers	
p120	82.4 (*n* = 199)
GM130	35.3 (*n* = 150)
Lava Lamp	28.7 (*n* = 115)
Endosomal markers	
Rbsn-5	9.1 (*n* = 132)
Rab5	9.3 (*n* = 97)
Rab7	0.9 (*n* = 114)
Rab11	15.7 (*n* = 261)

Fig. 2. GFP-Mon2 resides on the Golgi and endosomes. (**A-E**) Distribution of GFP-Mon2 (green) in stage 8 (A), stage 9 (B) and stage 10b (C,E) *Drosophila* oocytes. (D) Osk at the posterior of the oocyte shown in C. (E) Merged image of C and D. Arrowheads indicate the posterior pole, where Osk was detected. DNA was counterstained with DAPI (cyan). Scale bars: 20 μm. (**F-L**) Distribution of GFP-Mon2 in S2 cells. Cells expressing GFP-Mon2 were stained for Golgi markers p120 (F), GM130 (G) and Lava Lamp (H), or endosomal markers Rbsn-5 (I), Rab5 (J), Rab7 (K) and Rab11 (L). Transfected cells displayed an average of 12.1±5.8 (*n*=120) GFP-Mon2-positive structures per cell. Arrowheads indicate colocalized signals of GFP-Mon2 and markers for Golgi or endosomes. Scale bar: 5 μm. (**M**) Colocalization frequency of GFP-Mon2 with Golgi and endosomal markers. *n* in parentheses for each measurement is the total number of Mon2 positive vesicles counted.

detected endogenous *Drosophila* Mon2 in the oocyte. We therefore examined the intracellular distribution of Mon2 by using a GFP-tagged protein. The GFP-tagged Mon2 was functional and rescued the *mon2* mutant, so that eggs from *mon2* GLCs expressing GFP-Mon2 developed normally into adults. We found that GFP-Mon2 produced punctate signals throughout the ooplasm at stage 8, and was abundant in the subcortical region of the oocyte during stages 9-10 in an Osk-independent manner (Fig. 2A-E and see Fig. S1 in the supplementary material). These distribution patterns in the oocyte are similar to those of Golgi and endosomal proteins (Lee and Cooley, 2007; Tanaka and Nakamura, 2008). Consistent with this observation, when GFP-Mon2 was expressed in *Drosophila* S2 cells, the signals accumulated on vesicular structures, most of which (>80%) stained for the Golgi protein p120 (Fig. 2F,M). Less (~30%) colocalization was seen with other Golgi markers GM130 and Lava Lamp (Fig. 2G,H,M). In addition, up to 16% of GFP-Mon2-containing structures were positive for Rab5, Rbsn-5 and Rab11, but not for Rab7 (Fig. 2I-M), indicating that GFP-Mon2 is also present on a subpopulation of endosomes. These results suggest that *Drosophila* Mon2 resides on a specific Golgi compartment and Golgi-derived vesicles such as endosomes, as is reported for its yeast homolog (Efe et al., 2005; Jochum et al., 2002).

Mon2 is required for actin remodeling in response to Osk

The posterior localization of pole plasm components depends on the organization of microtubules along the anterior-posterior axis of the oocyte (Steinhauer and Kalderon, 2006). To determine whether microtubule alignment was affected in the *mon2* oocyte, we used kinesin-β-galactosidase (kin-β-gal), a microtubule plus-end marker that normally accumulates at the oocyte posterior during stages 9-10b (Fig. 3A) (Clark et al., 1994). Posterior kin-β-gal accumulation was normal in *mon2* GLC oocytes (Fig. 3B); therefore, it is unlikely that the failure to maintain pole plasm components at the posterior was due to aberrant microtubule organization.

Because Osk-induced endocytic cycling is required to anchor pole plasm components to the cortex (Tanaka and Nakamura, 2008), we next examined whether the endocytic pathway was affected in the *mon2* GLC oocytes. Osk-induced endocytic activity in the oocyte can be evaluated by the preferential internalization of a fluorescent lipophilic dye, FM4-64, from the posterior (Fig. 3C), and by the posterior accumulation of endosomal proteins, such as Rab5, Rab7 and Rab11 (Fig. 3E,G,I). These were normal in *mon2* oocytes (Fig. 3D,F,H,J). Furthermore, Osk misexpressed at the anterior in *mon2* oocytes recruited endosomal proteins to the ectopic site, as it did in otherwise wild-type oocytes (Fig. 3K-N; data not shown). These results indicate that Mon2 is not required for the Osk-induced activation of the endocytic pathway.

Osk is known to induce long F-actin projections, which are thought to anchor pole plasm components to the cortex (Fig. 4A,B) (Tanaka and Nakamura, 2008; Vanzo et al., 2007). In the *mon2* oocyte, however, F-actin projections did not form (Fig. 4C). Although a significant amount of Osk was detected at the posterior pole in stage 10b *mon2* oocytes, it was not tightly anchored there, but had detached from the cortical F-actin layer (Fig. 4C). We also examined the effects of ectopic Osk on actin remodeling at the anterior pole region of *mon2* oocytes (Fig. 4G-J). In wild-type oocytes, Osk overexpression at the anterior induced long F-actin projections (Fig. 4G,H). In *mon2* oocytes, however, the ectopic Osk induced faintly labeled, F-actin structures showing punctate labeling (Fig. 4I,J). Although abundant Osk was detected at the

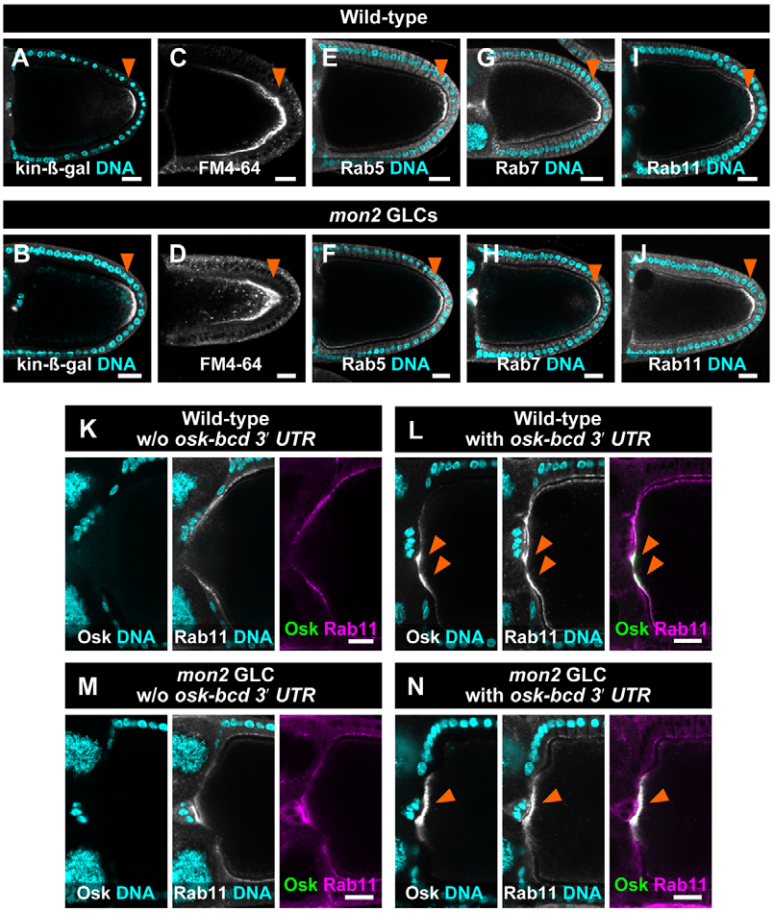

Fig. 3. Mon2 is not essential for microtubule array polarization or endocytic activity. (**A-J**) Localization of kin-β-gal (A,B), incorporated FM4-64 (C,D), Rab5 (E,F), Rab7 (G,H) and Rab11 (I,J) in stage 10a wild-type (A,C,E,G,I) and *mon2* (B,D,F,H,J) *Drosophila* oocytes. The posterior pole of the *mon2* GLC oocytes (arrowheads) showed normal enrichment of kin-β-gal, FM4-64 and endosomal proteins. (**K-N**) Rab11 localization in stage 10b wild-type (K,L) and *mon2* (M,N) oocytes without (K,M) or with (L,N) anterior Osk misexpression. Arrowheads indicate the ectopic Osk at the anterior oocyte pole. DNA was labeled with DAPI (cyan). Scale bars: 20 μm.

anterior of these oocytes, it was diffusely distributed towards the ooplasm (Fig. 4H,J). These data indicate that although Mon2 is dispensable in Osk-dependent alterations of F-actin structures per se, it is crucial in proper actin remodeling to form long F-actin projections from the oocyte cortex.

Genetic interactions between *mon2* and *rab5*

We previously reported that Osk-dependent actin remodeling in the oocyte requires a Rab5 effector protein, Rbsn-5 (Tanaka and Nakamura, 2008). In oocytes lacking Rbsn-5, aberrant F-actin aggregates form when Osk is misexpressed at the anterior pole, allowing pole plasm components to diffuse into the ooplasm. Similarly, in the absence of Rab5, ectopic Osk induced huge masses of aberrant F-actin aggregates in the ooplasm (Fig. 4K,L).

Intriguingly, although the cortical F-actin layer was disrupted at the posterior pole in stage 10b *rab5* oocytes (Fig. 4D), when we generated *rab5* GLCs in the *osk* mutant background, the cortical F-actin layer was restored (Fig. 4B,E). The *rab5 osk* double-mutant oocytes failed to form long F-actin projections at the posterior pole, as observed in *osk* oocytes (Fig. 4B,E). These results indicate that the disorganization of cortical F-actin bundles at the *rab5* oocyte posterior pole is dependent on Osk activity.

The above results showed that mutations in both *rab5* and *mon2* affect Osk-induced actin remodeling. As the polarized endocytic activity in *mon2* oocytes was normal (Fig. 3), we supposed that Mon2 might act downstream of, or parallel to, Rab5 in Osk-induced actin remodeling. We therefore generated a *mon2 rab5* double mutant to address their epistatic order. We found that the simultaneous loss of *mon2* and *rab5* suppressed the disorganization of the cortical F-actin bundles observed in *rab5* oocytes (Fig. 4F). Furthermore, as in *mon2* or *osk* oocytes, no long F-actin projections were induced in the *rab5 mon2* double-mutant oocytes (Fig. 4A-F). Although Osk was detected at the posterior pole of stage 10b *rab5 mon2* double-mutant oocytes, it was detached from the cortical F-actin layer and distributed diffusely (Fig. 4A,F). Similarly, the formation of aberrant F-actin aggregates induced by the anterior misexpression of Osk in *rab5* oocytes was, for the most part, suppressed by the simultaneous loss of Mon2 (Fig. 4K-N). No long F-actin projections were induced in the double-mutant oocyte, and the anteriorly expressed Osk was diffused into the ooplasm (Fig. 4N). Therefore, the double-mutant behaved like the *mon2* mutant. These data indicate that Mon2 is a downstream component of the Osk- and endocytosis-dependent pathway for actin remodeling and pole plasm anchoring.

Mon2 forms a complex with the actin nucleators Cappuccino and Spire

To identify proteins that might function with Mon2 in actin remodeling and pole plasm anchoring, we screened for Mon2 binding partners using the yeast two-hybrid system. Full-length *Drosophila* Mon2 was used as bait to screen a *Drosophila* ovarian cDNA library. From the screen, we recovered a C-terminal fragment of Spir (corresponding to amino acids 808-1020 of the Spir-A isoform; see Fig. S2 in the supplementary material). We further found that the middle part of Mon2 (amino acids 723-1160), which contains one of two ARM repeat domains, was sufficient for interaction with full-length Spir in the two-hybrid assay (Fig. 5A,B).

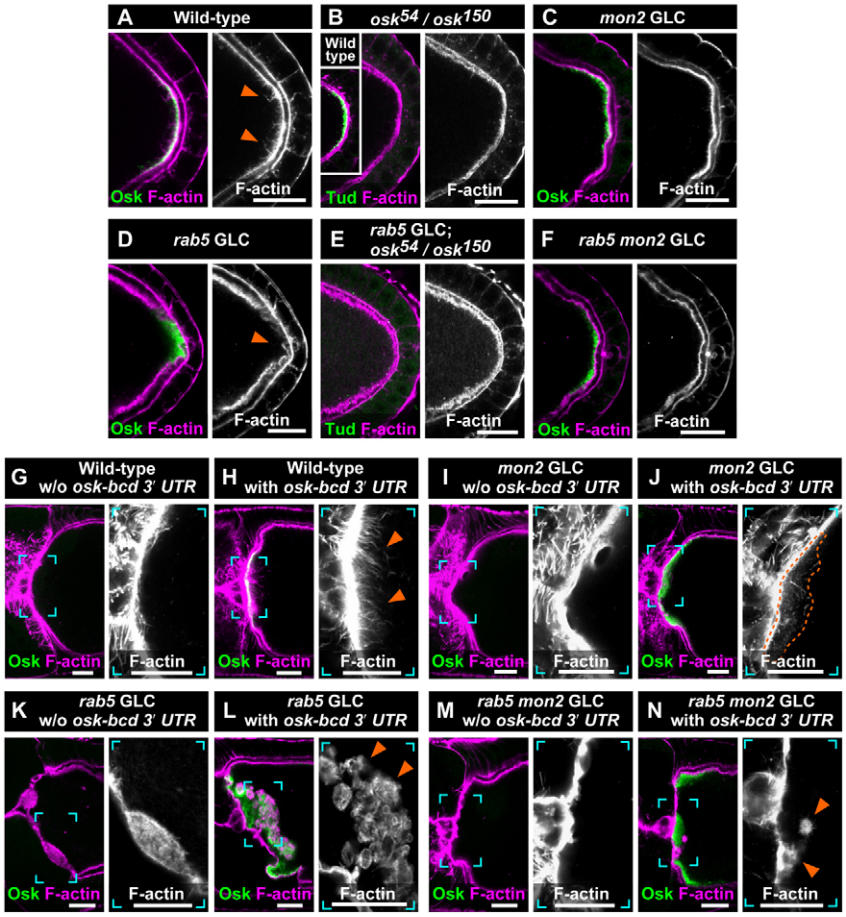

Fig. 4. Mon2 acts downstream of Rab5 for actin remodeling and pole plasm anchoring. (**A-F**) Posterior region of stage 10b *Drosophila* oocytes stained for Osk and F-actin (A,C,D,F), or Tudor (Tud) and F-actin (B,E) in wild-type (A), osk^{54}/osk^{150} *trans*-heterozygote (B), *mon2* GLC (C), *rab5* GLC (D), *rab5* GLC in osk^{54}/osk^{150} background (E) and *rab5 mon2* double-mutant GLC (F). Inset in B shows the Osk-dependent posterior localization of Tud in a wild-type oocyte. As osk^{54}/osk^{150} *trans*-heterozygotes produce non-functional Osk, mutant oocytes were identified by the posterior Tud loss. Arrowheads in A indicate posterior F-actin projections in wild-type oocytes. Arrowhead in D points to disorganized cortical F-actin bundles in the *rab5* oocyte. (**G-N**) Anterior of stage 10b oocytes stained for Osk and F-actin without (G,I,K,M) or with (H,J,L,N) anterior ectopic Osk in wild-type (G,H), *mon2* GLC (I,J), *rab5* GLC (K,L) and *rab5 mon2* double-mutant GLC (M,N) oocytes. In panel H, Osk and cortical F-actin are overlapping (shown in white). Enlargements of bracketed regions are shown on the right. Whereas ectopic Osk induced long F-actin projections in the wild-type oocyte (arrowheads in H), it induced aberrant F-actin aggregates or faint F-actin granules in the *rab5* GLC (arrowheads in L) or *mon2* GLC oocyte (the enclosed region with a dashed line in J), respectively. A few F-actin aggregates were detected by the Osk expression at the anterior pole of the *rab5 mon2* double-mutant oocyte (arrowheads in N). For each genotype, at least 20 mutant oocytes were examined. Scale bars: 20 μm.

Spir is a multidomain protein containing four tandem Wiskott-Aldrich syndrome protein (WASP) homology 2 (WH2) domains (see Fig. S2 in the supplementary material), which bind actin monomers consecutively to assemble actin filaments from their pointed ends (Qualmann and Kessels, 2009). The kinase noncatalytic C-lobe domain (KIND) of Spir is known to interact with Capu, a Formin-family protein that nucleates actin filaments from their barbed ends (Quinlan et al., 2007) (see Fig. S2 in the supplementary material). Spir also contains the Spir-box, a potential Rab-binding domain, and a modified FYVE (Fab1p, YOTB, Vac1p and EEA1) domain, which might interact with phosphatidylinositides, suggesting that Spir resides on vesicles (Kerkhoff et al., 2001). The C-terminal region of Spir contains a Jun N-terminal kinase (JNK) binding site (Otto et al., 2000), which was within the region sufficient for interaction with Mon2 in the yeast two-hybrid assay (see Fig. S2 in the supplementary material).

To examine whether Mon2 interacts with Spir in *Drosophila* cells, we conducted co-immunoprecipitation assays using lysates from S2 cells expressing GFP-Mon2 and 3×FLAG-Spir. We observed the specific co-immunoprecipitation of Spir with Mon2 from the lysates (Fig. 5C). In addition, although we did not detect any interaction between Mon2 and Capu in the yeast two-hybrid assay (data not shown), Capu was specifically co-immunoprecipitated with Mon2 from S2 cell lysates co-expressing GFP-Mon2 and 3×FLAG-Capu (Fig. 5D). Thus, Mon2 is likely to form a ternary complex with Capu and Spir in *Drosophila* cells.

Capu and Spir cooperatively promote the formation of long F-actin projections in response to Osk

We next examined whether Capu and Spir were required to form Osk-induced long F-actin projections in oocytes. *capu* and *spir* were originally identified as mutants with nearly identical defects in oocyte anterior-posterior axis formation (Schüpbach and Wieschaus, 1991). We isolated new alleles of *capu* and *spir* in our screen for mutants defective in GFP-Vas localization (see Fig. S2 in the supplementary material) (Tanaka and Nakamura, 2008). Oocytes lacking Capu or Spir show premature microtubule-based ooplasmic streaming, which normally starts at stage 10b (Dahlgaard et al., 2007; Theurkauf, 1994). This premature streaming perturbs the polarization of the microtubule array and the posterior localization of *osk* RNA. Because of these early defects in *osk* RNA localization during pole plasm assembly, the possible involvement of Capu and Spir in the Osk-dependent formation of long F-actin projections has never been investigated.

To overcome this problem, we expressed Osk ectopically at the anterior pole of *capu* or *spir* oocytes, and examined its effects on actin remodeling. In both mutant oocytes, the cortical F-actin layer at the anterior pole of stage 10b oocytes was indistinguishable from that of wild type (see Fig. S3 in the supplementary material). In contrast to wild-type oocytes, the anterior expression of Osk in these mutant oocytes induced disorganized, fuzzy ball-like F-actin structures (Fig. 6A-C). On the other hand, no fuzzy ball-like F-actin structures were induced by ectopic Osk in *capu spir* double-mutant oocytes (Fig. 6D). Considering their cooperative roles

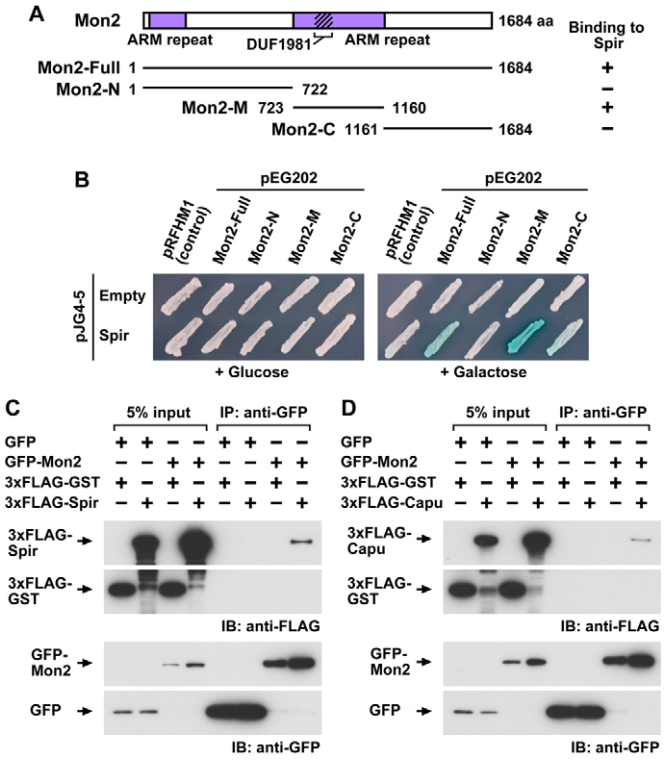

Fig. 5. Mon2 forms a complex with Capu and Spir. (**A**) Diagram of the *Drosophila* Mon2 protein. The ARM repeats and the DUF1981 domain are depicted by purple boxes and oblique lines, respectively. Full-length Mon2 (Mon2-Full) and the illustrated Mon2 fragments were used to map the Mon2 domain that interacts with Spir. (**B**) Yeast two-hybrid assays for interactions between Mon2 and Spir. Bait proteins were expressed under a constitutive promoter, and prey proteins under a galactose-inducible promoter. β-Galactosidase activity (green) was observed in cells co-expressing Spir with Mon2-Full or Mon2-M, but not with Mon2-N or a control, pRFHM1, in the presence of galactose. A weak interaction of Mon2-C with Spir did not support yeast growth in a medium lacking leucine (data not shown). Each interaction was tested using at least three independent transformants. (**C**,**D**) Mon2 interaction with Spir (C) or Capu (D). Lysates from S2 cells co-expressing the indicated proteins were immunoprecipitated with anti-GFP antibody and immunoblotted with anti-FLAG or anti-GFP antibody. FLAG-Spir (C) or FLAG-Capu (D) was specifically immunoprecipitated with GFP-Mon2, but not with GFP tag alone.

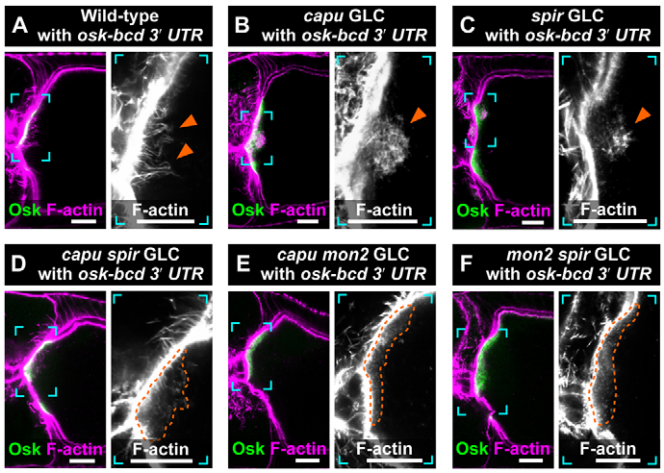

Fig. 6. Capu and Spir promote F-actin projection formation in response to Osk. (**A-F**) Anterior pole region of stage 10b *Drosophila* oocytes with ectopic Osk at the anterior, stained for Osk and F-actin. Wild type (A), *capu* GLC (B), *spir* GLC (C), *capu spir* double-mutant GLC (D), *capu mon2* double-mutant GLC (E) and *mon2 spir* double-mutant GLC (F). Enlargements of the bracketed regions are shown on the right. Ectopic Osk induced long F-actin projections in wild-type oocytes (arrowheads in A). By contrast, it induced fuzzy ball-like F-actin structures in the *capu* or *spir* oocytes (arrowheads in B,C), but no fuzzy ball-like F-actin structures in *capu spir* double-mutant oocytes (D). In *capu spir*, *capu mon2* and *mon2 spir* double-mutant oocytes, ectopic Osk induced faint F-actin granules (the enclosed regions with a dashed line in D-F), as observed in the *mon2* oocyte (see Fig. 4J). For each genotype, at least 20 mutant oocytes were examined. Scale bars: 20 μm. (See also Fig. S3 in the supplementary material.)

during oocyte axis establishment (Dahlgaard et al., 2007), it is likely that the fuzzy ball-like structures are intermediates between the long F-actin projections, as seen in wild-type background, and faint F-actin granules in the *capu spir* double-mutant. The ectopic Osk was not tightly anchored at the anterior pole of the oocyte, but had detached from the cortical F-actin layer (Fig. 6A-D). These data indicate that Capu and Spir cooperatively remodel the cortical actin cytoskeleton in response to Osk and are involved in pole plasm anchoring.

To investigate further the functional relationships between Mon2 and Capu or Spir, we generated *capu mon2* and *mon2 spir* double-mutant oocytes and analyzed the effects of ectopic anterior Osk expression on actin remodeling in these oocytes. In both *capu mon2* and *mon2 spir* double-mutant oocytes, Osk expressed at the anterior did not induce either fuzzy ball-like F-actin structures or F-actin projections (Fig. 6E,F). Instead, ectopic Osk induced faint F-actin granules in these double-mutant oocytes, indicating that the double-mutants behaved like the *mon2* single-mutant (Fig. 4J). Because Capu and Spir directly regulate actin dynamics, the genetic interactions we detected provide compelling evidence that Mon2 instructs Capu and Spir to form long F-actin projections in response to Osk.

Mon2 is required for the accumulation of Rho1 GTPase at the oocyte posterior

Capu and Spir both interact with Rho1, a conserved small GTPase (Rosales-Nieves et al., 2006). We therefore examined whether Rho1 is required in forming Osk-dependent F-actin projections. Because *rho1*-null GLCs are non-viable, we developed oocytes with significantly reduced levels of Rho1 by generating trans-heterozygotes of mutations for *rho1* and *wimp* (*RpII140* – FlyBase), which encodes an RNA polymerase II subunit (Magie et al., 1999) (hereafter, 'reduced-*rho1*' oocytes). Consistent with the known role of Rho1 in organizing cortical F-actin bundles in late-stage oocytes and early embryos (Magie et al., 1999; Rosales-Nieves et al., 2006), few F-actin projections were induced at the posterior pole in reduced-*rho1* oocytes. Although a substantial amount of Osk was detected at the oocyte posterior, it was distributed diffusely (Fig. 7A,B), indicating that Rho1 is required for cortical anchoring of the pole plasm. These results suggest that Capu, Spir and Rho1 are all required for actin remodeling during the assembly and anchorage of the pole plasm at the posterior pole of the oocyte.

We also found that when wild-type ovaries were stained with an anti-human Rho monoclonal antibody (3L74), the posterior region of stage 10b oocytes were enriched with immunosignal

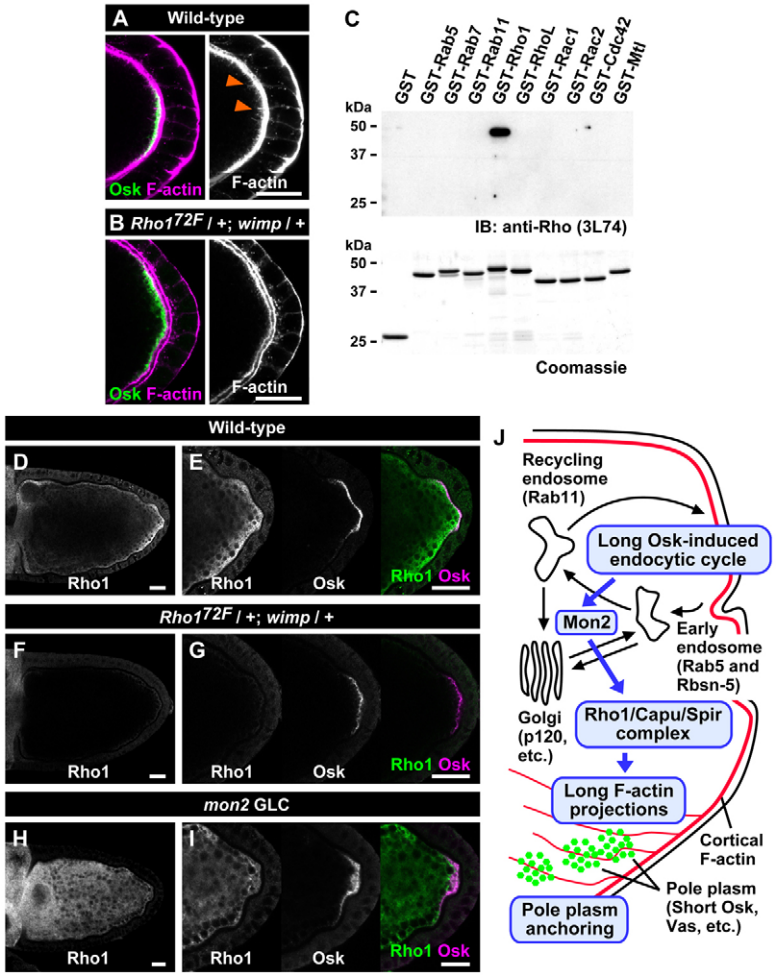

Fig. 7. Mon2 is required for posterior accumulation of Rho1. (**A**,**B**) Posterior region of wild-type (A) and reduced-*rho1* (B) stage 10b *Drosophila* oocytes stained for Osk and F-actin. Long F-actin projections were observed in wild-type oocytes (arrowheads in A). By contrast, few F-actin projections were detected in reduced-*rho1* oocytes (B). Note that Osk protein in the reduced-*rho1* oocyte was diffuse. (**C**) The 3L74 antibody reacted specifically with GST-*Drosophila* Rho1, but not RhoL, Rac1, Rac2, Cdc42, Mtl, Rab5, Rab7 or Rab11. 100 ng of each GST fusion protein was loaded for immunoblot analysis, and 3 μg for Coomassie staining. (**D-I**) Rho1 localization in stage 10b wild-type (D,E), reduced-*rho1* (F,G) and *mon2* (H,I) oocytes. (E,G,I) Magnified posterior region shown in D, F and H, respectively, with images of Osk staining. For each genotype, at least 20 mutant oocytes were examined. Scale bars: 20 μm. (**J**) A proposed model of pole plasm anchoring to the posterior cortex of the oocyte. Osk upregulates endocytosis at the oocyte posterior, producing 'specialized' vesicles on which Mon2 resides. The Mon2 on these vesicles regulates the assembly and/or the activity of the complex containing Rho1, Capu and Spir to promote the formation of long F-actin projections, which restricts the pole plasm to the oocyte cortex.

(Fig. 7D,E). The 3L74 antibody was raised against a peptide with a sequence highly conserved with *Drosophila* Rho1 (21 out of 22 identical amino acids). We confirmed that, of six Rho-family and three Rab-family GTPases in the *Drosophila* genome, the 3L74 antibody specifically reacted with only Rho1 (Fig. 7C). As further confirmation of its specificity, the antibody did not produce posterior signals in reduced-*rho1* oocytes (Fig. 7F,G). Interestingly, the posterior enrichment of Rho1 signals was lost in the *mon2* oocyte (Fig. 7H,I). Although no direct interaction between Mon2 and Rho1 was detected in the yeast two-hybrid assay (data not shown), these results support the idea that in response to Osk, Mon2 is a scaffold protein that instructs the Capu-Spir-Rho1 complex to form long F-actin projections, which anchor the pole plasm components at the oocyte cortex (Fig. 7J).

DISCUSSION

Osk-dependent actin regulators required for cortical anchoring of the pole plasm

We found that Capu and Spir act together to form long F-actin projections and to anchor pole plasm components at the oocyte cortex, and that Mon2 is essential to these processes (Fig. 6). Capu and Spir also regulate the timing for initiating ooplasmic streaming and microtubule array polarization in the oocyte (Qualmann and Kessels, 2009). However, the polarity of microtubule arrays was not affected in *mon2* oocytes (Fig. 3). Therefore, Mon2 is not always required for Capu and Spir to function. Rather, it appears to regulate specifically these actin nucleators through the Osk-induced endocytic pathway.

Mon2 is required for the formation of Osk-induced long F-actin projections at the oocyte posterior. Interestingly, ectopic overexpression of Osk at the anterior pole in the *mon2* oocyte induced granular, albeit faint, F-actin structures (Fig. 4), indicating that Osk-induced actin remodeling does not totally cease in the *mon2* oocyte. Ectopic Osk at the anterior of *capu spir* double-mutant oocytes also induced faint F-actin granules in the cytoplasm (Fig. 6). Thus, additional, as yet uncharacterized, actin regulators appear to function in response to Osk. Notably, two actin-binding proteins, Bifocal and Homer, play redundant roles in anchoring Osk to the cortex (Babu et al., 2004). Although the precise roles of Bifocal and Homer in this process remain elusive, they might function independently of Mon2.

Mon2 couples endocytic activity with cortical actin remodeling

Oocytes lacking Rab5 showed disrupted posterior cortical F-actin bundles, which was suppressed by the simultaneous loss of Osk (Fig. 4). These results reconfirm that the endocytic pathway needs intact Osk function for actin remodeling (Tanaka and Nakamura, 2008). We also found that the F-actin disorganization in *rab5* oocytes is Mon2-dependent (Fig. 4). Therefore, Mon2 can facilitate actin remodeling even when Rab5 is absent, but endosomal

trafficking, in which Rab5 is involved, is crucial for regulating Mon2. Mammalian Rab5 is also involved in actin remodeling (Lanzetti et al., 2004; Palamidessi et al., 2008). For example, Rac1 GTPase, a regulator of F-actin dynamics, is activated by Rab5-dependent endocytosis, and the local activation of Rac1 on early endosomes and its subsequent recycling to the plasma membrane spatially regulate actin remodeling (Palamidessi et al., 2008). Thus, local endocytic cycling provides a specific platform for actin remodeling in a wide range of cell types.

There is growing evidence that endosomes act as multifunctional platforms for many types of molecular machinery (Gould and Lippincott-Schwartz, 2009). Intriguingly, Mon2 is located on the Golgi and endosomes, without entirely accumulating at the oocyte posterior. We therefore propose that the Osk-induced stimulation of endocytic cycling at the oocyte posterior leads to the formation of specialized vesicles, which instruct a fraction of Mon2 to regulate the activity of Capu, Spir and Rho1 to form long F-actin projections from the cortex. Although the functional property of Osk-induced endocytic vesicles has yet to be ascertained, long Osk is known to associate with the surface of endosomes (Vanzo et al., 2007). Therefore, long Osk might modify endosome specificity to recruit and/or stabilize the machineries responsible for actin remodeling.

Oocytes lacking Mon2 can mature without morphological abnormalities, but their eggs are nonviable. Furthermore, *Drosophila mon2* mutations show recessive lethality, indicating that Mon2 has additional functions in somatic cell development. It might function in regulating vesicle trafficking or protein targeting, as reported in yeasts (Efe et al., 2005; Gillingham et al., 2006; Jochum et al., 2002; Singer-Krüger et al., 2008; Wicky et al., 2004). As vesicle trafficking is often linked with establishing and maintaining cell polarity (Gould and Lippincott-Schwartz, 2009; Shivas et al., 2010), it is an attractive idea that Mon2 might regulate the polarity protein localization and/or mediate the signal transduction for cell polarization in somatic cells, as well as in germ cells. Supporting this idea, a Mon2 homolog in *C. elegans* has been implicated in the asymmetric division of epithelial stem cells (Kanamori et al., 2008).

Positive-feedback loops during pole plasm assembly through local endocytic activation

It has been proposed that long Osk localizes to the endosomal membrane and generates a positive-feedback loop for cortical anchoring of pole plasm components (Vanzo et al., 2007). Osk is also thought to generate another positive-feedback loop to maintain the polarity of microtubule arrays, and the process appears to be endosomal protein-dependent (Tanaka and Nakamura, 2008; Zimyanin et al., 2007). Although Rbsn-5 is required for both feedback loops (Tanaka and Nakamura, 2008), Mon2 acts specifically in the loop regulating actin remodeling for pole plasm anchoring, indicating that the two feedback loops are regulated by distinct mechanisms. The endocytic pathway consists of multiple vesicle trafficking steps, including endocytosis, endosomal recycling, late-endosomal sorting and endosome-to-Golgi trafficking. Therefore, determining which steps in the endocytic pathway are used by the two Osk-dependent positive-feedback loops is an important aim for future exploration.

Acknowledgements

We thank A. Ephrussi, S. Goto, J. Großhans, A. Guichet, J. C. Sisson, D. St Johnston, and the Bloomington and Kyoto *Drosophila* Stock Centers for reagents and fly strains. We also thank S. L. Bullock, Y. Kageyama, B. P. Muthusamy, T. Otani, I. M. Palacios, D. St Johnston, R. Suyama, and T. Uemura for critical reading of the manuscript. This work was supported in part by a Grant-in-Aid from the Ministry of Education, Culture, Sports and Science, Japan (MEXT) and the Japan Society for the Promotion of Science (JSPS).

Competing interests statement

The authors declare no competing financial interests.

Supplementary material

Supplementary material for this article is available at
http://dev.biologists.org/lookup/suppl/doi:10.1242/dev.062208/-/DC1

References

Amikura, R., Hanyu, K., Kashikawa, M. and Kobayashi, S. (2001). Tudor protein is essential for the localization of mitochondrial RNAs in polar granules of *Drosophila* embryos. *Mech. Dev.* **107**, 97-104.

Babu, K., Cai, Y., Bahri, S., Yang, X. and Chia, W. (2004). Roles of Bifocal, Homer, and F-actin in anchoring Oskar to the posterior cortex of *Drosophila* oocytes. *Genes Dev.* **18**, 138-143.

Breitwieser, W., Markussen, F. H., Horstmann, H. and Ephrussi, A. (1996). Oskar protein interaction with Vasa represents an essential step in polar granule assembly. *Genes Dev.* **10**, 2179-2188.

Cha, B. J., Serbus, L. R., Koppetsch, B. S. and Theurkauf, W. E. (2002). Kinesin I-dependent cortical exclusion restricts pole plasm to the oocyte posterior. *Nat. Cell Biol.* **4**, 592-598.

Clark, I., Giniger, E., Ruohola-Baker, H., Jan, L. Y. and Jan, Y. N. (1994). Transient posterior localization of a kinesin fusion protein reflects anteroposterior polarity of the *Drosophila* oocyte. *Curr. Biol.* **4**, 289-300.

Dahlgaard, K., Raposo, A. A., Niccoli, T. and St Johnston, D. (2007). Capu and Spire assemble a cytoplasmic actin mesh that maintains microtubule organization in the *Drosophila* oocyte. *Dev. Cell* **13**, 539-553.

Dollar, G., Struckhoff, E., Michaud, J. and Cohen, R. S. (2002). Rab11 polarization of the *Drosophila* oocyte: a novel link between membrane trafficking, microtubule organization, and *oskar* mRNA localization and translation. *Development* **129**, 517-526.

Efe, J. A., Plattner, F., Hulo, N., Kressler, D., Emr, S. D. and Deloche, O. (2005). Yeast Mon2p is a highly conserved protein that functions in the cytoplasm-to-vacuole transport pathway and is required for Golgi homeostasis. *J. Cell Sci.* **118**, 4751-4764.

Ephrussi, A. and Lehmann, R. (1992). Induction of germ cell formation by *oskar*. *Nature* **358**, 387-392.

Gillingham, A. K., Whyte, J. R., Panic, B. and Munro, S. (2006). Mon2, a relative of large Arf exchange factors, recruits Dop1 to the Golgi apparatus. *J. Biol. Chem.* **281**, 2273-2280.

Gould, G. W. and Lippincott-Schwartz, J. (2009). New roles for endosomes: from vesicular carriers to multi-purpose platforms. *Nat. Rev. Mol. Cell Biol.* **10**, 287-292.

Jankovics, F., Sinka, R. and Erdélyi, M. (2001). An interaction type of genetic screen reveals a role of the *Rab11* gene in *oskar* mRNA localization in the developing *Drosophila melanogaster* oocyte. *Genetics* **158**, 1177-1188.

Jankovics, F., Sinka, R., Lukácsovich, T. and Erdélyi, M. (2002). MOESIN crosslinks actin and cell membrane in *Drosophila* oocytes and is required for OSKAR anchoring. *Curr. Biol.* **12**, 2060-2065.

Jochum, A., Jackson, D., Schwarz, H., Pipkorn, R. and Singer-Krüger, B. (2002). Yeast Ysl2p, homologous to Sec7 domain guanine nucleotide exchange factors, functions in endocytosis and maintenance of vacuole integrity and interacts with the Arf-Like small GTPase Arl1p. *Mol. Cell. Biol.* **22**, 4914-4928.

Kanamori, T., Inoue, T., Sakamoto, T., Gengyo-Ando, K., Tsujimoto, M., Mitani, S., Sawa, H., Aoki, J. and Arai, H. (2008). β-Catenin asymmetry is regulated by PLA1 and retrograde traffic in *C. elegans* stem cell divisions. *EMBO J.* **27**, 1647-1657.

Kerkhoff, E., Simpson, J. C., Leberfinger, C. B., Otto, I. M., Doerks, T., Bork, P., Rapp, U. R., Raabe, T. and Pepperkok, R. (2001). The Spir actin organizers are involved in vesicle transport processes. *Curr. Biol.* **11**, 1963-1968.

Kim-Ha, J., Smith, J. L. and Macdonald, P. M. (1991). *oskar* mRNA is localized to the posterior pole of the *Drosophila* oocyte. *Cell* **66**, 23-35.

Lanzetti, L., Palamidessi, A., Areces, L., Scita, G. and Di Fiore, P. P. (2004). Rab5 is a signalling GTPase involved in actin remodelling by receptor tyrosine kinases. *Nature* **429**, 309-314.

Lee, S. and Cooley, L. (2007). Jagunal is required for reorganizing the endoplasmic reticulum during *Drosophila* oogenesis. *J. Cell Biol.* **176**, 941-952.

Magie, C. R., Meyer, M. R., Gorsuch, M. S. and Parkhurst, S. M. (1999). Mutations in the Rho1 small GTPase disrupt morphogenesis and segmentation during early *Drosophila* development. *Development* **126**, 5353-5364.

Mahowald, A. P. (2001). Assembly of the *Drosophila* germ plasm. *Int. Rev. Cytol.* **203**, 187-213.

Markussen, F. H., Michon, A. M., Breitwieser, W. and Ephrussi, A. (1995). Translational control of *oskar* generates short OSK, the isoform that induces pole plasm assembly. *Development* **121**, 3723-3732.

Murén, E., Oyen, M., Barmark, G. and Ronne, H. (2001). Identification of yeast deletion strains that are hypersensitive to brefeldin A or monensin, two drugs that affect intracellular transport. *Yeast* **18**, 163-172.
Otto, I. M., Raabe, T., Rennefahrt, U. E., Bork, P., Rapp, U. R. and Kerkhoff, E. (2000). The p150-Spir protein provides a link between c-Jun N-terminal kinase function and actin reorganization. *Curr. Biol.* **10**, 345-348.
Palamidessi, A., Frittoli, E., Garré, M., Faretta, M., Mione, M., Testa, I., Diaspro, A., Lanzetti, L., Scita, G. and Di Fiore, P. P. (2008). Endocytic trafficking of Rac is required for the spatial restriction of signaling in cell migration. *Cell* **134**, 135-147.
Parkhurst, S. M. and Ish-Horowicz, D. (1991). *wimp*, a dominant maternal-effect mutation, reduces transcription of a specific subset of segmentation genes in *Drosophila*. *Genes Dev.* **5**, 341-357.
Polesello, C., Delon, I., Valenti, P., Ferrer, P. and Payre, F. (2002). Dmoesin controls actin-based cell shape and polarity during *Drosophila melanogaster* oogenesis. *Nat. Cell Biol.* **4**, 782-789.
Qualmann, B. and Kessels, M. M. (2009). New players in actin polymerization – WH2-domain-containing actin nucleators. *Trends Cell Biol.* **19**, 276-285.
Quinlan, M. E., Hilgert, S., Bedrossian, A., Mullins, R. D. and Kerkhoff, E. (2007). Regulatory interactions between two actin nucleators, Spire and Cappuccino. *J. Cell Biol.* **179**, 117-128.
Rosales-Nieves, A. E., Johndrow, J. E., Keller, L. C., Magie, C. R., Pinto-Santini, D. M. and Parkhurst, S. M. (2006). Coordination of microtubule and microfilament dynamics by *Drosophila* Rho1, Spire and Cappuccino. *Nat. Cell Biol.* **8**, 367-376.
Sano, H., Nakamura, A. and Kobayashi, S. (2002). Identification of a transcriptional regulatory region for germline-specific expression of *vasa* gene in *Drosophila melanogaster*. *Mech. Dev.* **112**, 129-139.
Schüpbach, T. and Wieschaus, E. (1991). Female sterile mutations on the second chromosome of *Drosophila melanogaster*. II. Mutations blocking oogenesis or altering egg morphology. *Genetics* **129**, 1119-1136.
Shivas, J. M., Morrison, H. A., Bilder, D. and Skop, A. R. (2010). Polarity and endocytosis: reciprocal regulation. *Trends Cell Biol.* **20**, 445-452.
Singer-Krüger, B. and Ferro-Novick, S. (1997). Use of a synthetic lethal screen to identify yeast mutants impaired in endocytosis, vacuolar protein sorting and the organization of the cytoskeleton. *Eur. J. Cell Biol.* **74**, 365-375.
Singer-Krüger, B., Lasić, M., Bürger, A. M., Hausser, A., Pipkorn, R. and Wang, Y. (2008). Yeast and human Ysl2p/hMon2 interact with Gga adaptors and mediate their subcellular distribution. *EMBO J.* **27**, 1423-1435.
Sisson, J. C., Field, C., Ventura, R., Royou, A. and Sullivan, W. (2000). Lava lamp, a novel peripheral golgi protein, is required for *Drosophila melanogaster* cellularization. *J. Cell Biol.* **13**, 905-918.
Smith, J. L., Wilson, J. E. and Macdonald, P. M. (1992). Overexpression of *oskar* directs ectopic activation of *nanos* and presumptive pole cell formation in Drosophila embryos. *Cell* **70**, 849-859.
Spradling, A. C. (1993). Development genetics of oogenesis. In *The Development of Drosophila melanogaster* (ed. M. Bate and A. Martinez-Arias), pp. 1-70. Cold Spring Harbor, NY: Cold Spring Harbor Laboratory Press.
Steinhauer, J. and Kalderon, D. (2006). Microtubule polarity and axis formation in the *Drosophila* oocyte. *Dev. Dyn.* **235**, 1455-1468.
Strutt, D. I., Weber, U. and Mlodzik, M. (1997). The role of RhoA in tissue polarity and Frizzled signalling. *Nature* **387**, 292-295.
Tanaka, T. and Nakamura, A. (2008). The endocytic pathway acts downstream of Oskar in *Drosophila* germ plasm assembly. *Development* **135**, 1107-1117.
Theurkauf, W. E. (1994). Premature microtubule-dependent cytoplasmic streaming in *cappuccino* and *spire* mutant oocytes. *Science* **265**, 2093-2096.
Vanzo, N. F. and Ephrussi, A. (2002). Oskar anchoring restricts pole plasm formation to the posterior of the *Drosophila* oocyte. *Development* **129**, 3705-3714.
Vanzo, N., Oprins, A., Xanthakis, D., Ephrussi, A. and Rabouille, C. (2007). Stimulation of endocytosis and actin dynamics by Oskar polarizes the *Drosophila* oocyte. *Dev. Cell* **12**, 543-555.
Wicky, S., Schwarz, H. and Singer-Krüger, B. (2004). Molecular interactions of yeast Neo1p, an essential member of the Drs2 family of aminophospholipid translocases, and its role in membrane trafficking within the endomembrane system. *Mol. Cell. Biol.* **24**, 7402-7418.
Wucherpfennig, T., Wilsch-Bräuninger, M. and González-Gaitán, M. (2003). Role of *Drosophila* Rab5 during endosomal trafficking at the synapse and evoked neurotransmitter release. *J. Cell Biol.* **161**, 609-624.
Yano, H., Yamamoto-Hino, M., Abe, M., Kuwahara, R., Haraguchi, S., Kusaka, I., Awano, W., Kinoshita-Toyoda, A., Toyoda, H. and Goto, S. (2005). Distinct functional units of the Golgi complex in *Drosophila* cells. *Proc. Natl. Acad. Sci. USA* **102**, 13467-13472.
Zimyanin, V., Lowe, N. and St Johnston, D. (2007). An Oskar-dependent positive feedback loop maintains the polarity of the *Drosophila* oocyte. *Curr. Biol.* **17**, 353-359.
Zimyanin, V. L., Belaya, K., Pecreaux, J., Gilchrist, M. J., Clark, A., Davis, I. and St Johnston, D. (2008). In vivo imaging of *oskar* mRNA transport reveals the mechanism of posterior localization. *Cell* **134**, 843-853.